

Aod2*, the Locus Controlling Development of Atrophy in Neonatal Thymectomy-induced Autoimmune Ovarian Dysgenesis, Co-localizes with *Il2*, *Fgfb*, and *Idd3

By Cory Teuscher,* Bryan B. Wardell,* Jared K. Lunceford,*
Sandra D. Michael,† and Kenneth S. K. Tung§

From the *Department of Microbiology, Brigham Young University, Provo, Utah 84602; †Department of Biological Sciences, State University of New York, Binghamton, New York 13902; and §Department of Pathology, University of Virginia School of Medicine, Charlottesville, Virginia 22908

Summary

In genetically susceptible strains of mice, such as A/J and (C57BL/6J × A/J)_{F1} hybrids, neonatal thymectomy-induced autoimmune ovarian dysgenesis (AOD) is characterized by the development of antiovarian autoantibodies, oophoritis, and atrophy. Temporally, atrophy may be observed during and after the regression of inflammatory infiltrates from the ovary. Histologically, lesions appear as areas devoid of ovarian follicles in all stages of development that have been replaced by luteinized interstitial cells. We report here the mapping of *Aod2*, the locus that controls this phenotype, to mouse chromosome 3 within a region encoding *Il2* and *Fgfb*. Most significant, however, is the co-localization of *Aod2* to *Idd3*, a susceptibility gene that plays a role in autoimmune insulin-dependent type 1 diabetes mellitus in the nonobese diabetic mouse.

Premature ovarian failure (POF)¹ has been recognized for some time as a cause of infertility in women, but the precise etiology of the disease remains ill defined. Both autoimmune and genetic components have been implicated in the disease process (1–6). With regard to autoimmunity, women with POF frequently present with antiovarian autoantibodies, ovarian lymphocytic infiltrates, and abnormalities in T cell subsets and lymphokine levels (1, 2). In addition, POF is observed in association with other organ-specific autoimmune disorders, such as type 1 and type 2 polyendocrinopathies, and immunosuppressive therapy has been successful at restoring normal ovarian function (1).

A genetic component in the etiology of POF has also been demonstrated in normal 46XX karyotype families (3–6). The familial nature of POF was documented across multiple generations in a number of kindreds and is consistent with an autosomal-dominant, sex-limited vertical transmission (5, 6). In fact, it has been suggested that this form of POF may not be as rare as believed because of previous failures to establish detailed menopausal histories on both sides of a patient's family (6).

A highly useful system for studying both the autoimmune and genetic components of POF is the day 3 thymectomy (D3Tx)-induced model of autoimmune ovarian dysgenesis (AOD) in mice (7–10). The D3Tx model of

AOD is unique in that disease induction depends exclusively on perturbation of the normal developing immune system, is T cell mediated, and is strain specific. For example, D3Tx A/J and (C57BL/6J × A/J)_{F1} hybrid mice are susceptible to AOD, whereas C57BL/6J mice are resistant (11). AOD is phenotypically characterized by the presence of antiovarian autoantibodies, ovarian lymphocytic infiltrates (oophoritis), and ovarian atrophy (7–10). Oophoritis is first observed in the ovaries of D3Tx mice at 3–4 wk after thymectomy and is presented as infiltration of the hilar region, which later extends into the interfollicular areas as well as within growing and antral follicles (7). Subsequently, the infiltrating cells may regress from the ovaries, which then become atrophic. Atrophic areas are devoid of ovarian follicles in all stages of development and are replaced by interstitial cells that appear luteinized.

Previously, we demonstrated that *Aod1*, the gene controlling the development of both the antiovarian autoantibody and T cell-mediated autoimmune responses after D3Tx, maps to chromosome 16 within a region encoding several loci of immunologic relevance (11). In contrast, however, the phenotypic expression of ovarian atrophy was not linked to *Aod1*. In this study, we report the identification and mapping of the gene controlling the phenotypic expression of atrophy to chromosome 3.

Materials and Methods

Animals. Female (C57BL/6J × A/J)_{F1} hybrid and male C57BL/6J mice were purchased from The Jackson Laboratory

¹Abbreviations used in this paper: AOD, autoimmune ovarian dysgenesis; D3Tx, day 3 thymectomy; IDDM, insulin-dependent diabetes mellitus; POF, premature ovarian failure.

(Bar Harbor, ME). (C57BL/6J × A/J)F₁ × C57BL/6J back-cross (BC1) mice were generated and D3Tx performed under ether anesthesia using a suction pipette technique (11). At 24 d of age, the animals were weaned and separated by sex. Animals were maintained on mouse pellets (Ralston-Purina, St. Louis, MO) and acidified water ad libitum. D3Tx females were killed at 60 d of age. Individual serum samples were obtained, the ovaries were collected for histopathologic analysis, and livers were snap frozen for the isolation of DNA (11, 12).

Histopathologic Analysis of Ovarian Atrophy. The ovaries of the D3Tx BC1 mice were fixed in Bouin's fixative and embedded in paraffin, and 5- μ m sections were stained with hematoxylin and eosin. Multiple-step sections were evaluated in a double-blind fashion and scored for oophoritis and atrophy as previously described (11).

DNA Isolation. Genomic DNA was isolated from liver tissue as previously described (11, 12). Briefly, 0.5 g of tissue, maintained in liquid nitrogen, was pulverized with a mortar and pestle. The cells were lysed and deproteinized with SDS and proteinase K, followed by phenol/chloroform/isoamyl alcohol extraction(s). The DNA was then precipitated in sodium acetate with isoamyl alcohol, suspended in TE (10 mM Tris-HCl, pH 7.4, 1 mM EDTA), reprecipitated with ammonium acetate and ethanol, and resuspended in TE. Working aliquots of all DNA samples were prepared by bringing them to the appropriate concentrations in TE' (10 mM Tris-HCl, pH 7.4, 0.1 mM EDTA) and then stored at 4°C.

Microsatellite Primers, Amplification Conditions, and Detection of PCR Products. Microsatellite primers were purchased from Research Genetics Incorporated (Huntsville, AL) or synthesized according to sequences obtained through the Whitehead Institute/MIT Mouse Genome Database (13). PCR parameters for microsatellite typing were performed as previously described (11–13). Microsatellite alleles were resolved by electrophoresis on large-format denaturing polyacrylamide gels and visualized by autoradiography on film (Eastman Kodak Co., Rochester, NY).

Linkage Analysis. 74 of the 144 animals studied exhibited autoimmune oophoritis (11). Of the 74 with oophoritis, 25 devel-

oped atrophy. This population was used for linkage analysis. Linkage of marker loci to atrophy was evaluated by χ^2 analysis against a predicted frequency of 1:1 for marker loci, with linkage significant at $P \leq 0.001$. Segregation distortion was examined by determining the genotype frequency of randomly selected marker loci distributed throughout the genome in the 144 D3Tx BC1 mice. In no case was significant distortion from the predicted frequency of 1:1 observed. The maximum likelihood positional estimate for the location of the *Aod2* locus on chromosome 3 was performed using the MAPMAKER program (14). Genome coverage was estimated by using the position of marker loci as reported on the Whitehead Institute/MIT Mouse Genome Database and applying a value of 20 cM on each side of the marker loci.

Results and Discussion

In mice with autoimmune oophoritis, the infiltrating cells may regress from the ovaries, which then become atrophic. Of the 74 D3Tx BC1 mice with oophoritis, 25 exhibited this phenotype (Fig. 1). To map the gene or genes that control atrophy, a linkage map was generated using the affected population and a panel of 131 microsatellites that distinguish C57BL/6J and A/J mice. This analysis revealed significant linkage of atrophy to marker loci on chromosome 3 (Table 1). Maximal linkage was seen on chromosome 3 to *D3Mit224*, *D3Mit63*, *D3Mit133*, *D3Mit226*, *D3Mit182*, *D3Mit227*, *D3Mit64*, *D3Mit5*, *D3Mit6*, and *D3Mit65* (all with $\chi^2 = 11.6$, $P = 0.0007$). We have designated this gene *Aod2*. Maximum likelihood estimates for the location of *Aod2* on chromosome 3 were carried out by multilocus linkage analysis (14). The results place *Aod2* within a 95% confidence interval bordered by *D3Mit21* (*Il2*) (LOD = 2.09) and *D3Mit154* (LOD = 2.09) at 16 and 25 cM from the centromere of chromosome 3, respectively.

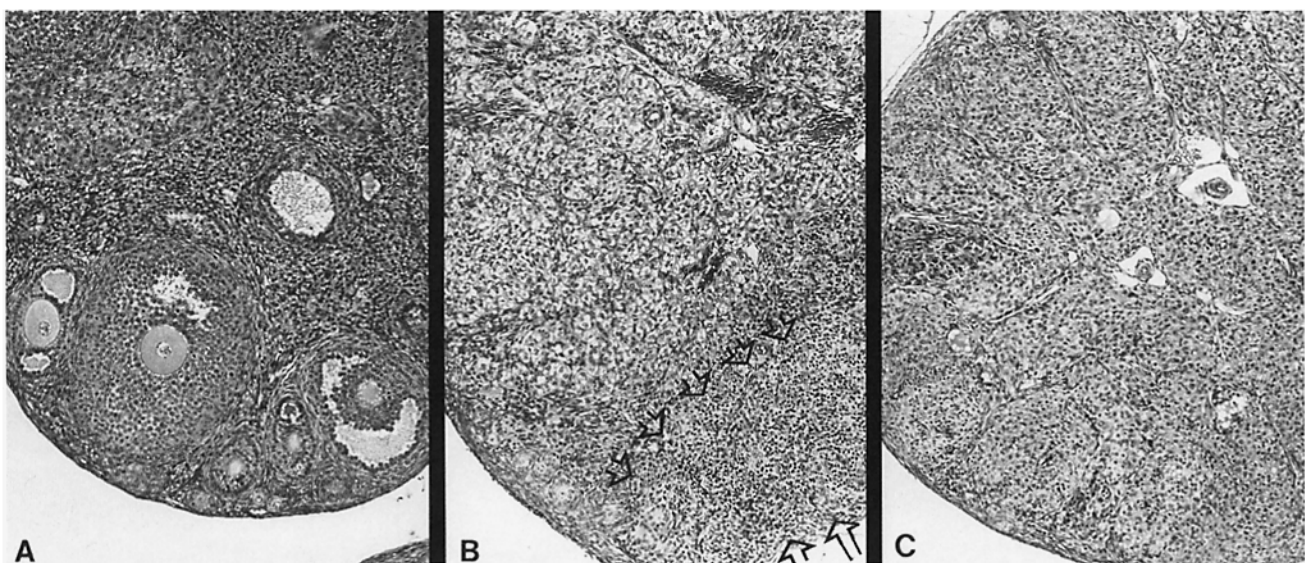


Figure 1. Progression from oophoritis to ovarian atrophy in D3Tx mice. (A) A normal ovary containing growing and antral follicles; (B) an atrophic ovary containing a large cluster of infiltrating lymphocytes (arrows); (C) an atrophic ovary with minimal inflammatory cells.

Table 1. Linkage Map of the Mouse Genome with Linkage of Marker Loci to Atrophy as a Function of Oophoritis*

Chromosome (cM) ^{2‡}	Locus	Atrophy		$\chi^2 \geq 4^{3§}$	P value
		Ho	He		
1 (8)	<i>D1Mit3</i>	13	11		
1 (18)	<i>D1Mit170</i>	10	14		
1 (45)	<i>D1Mit46</i>	13	11		
1 (67)	<i>D1Nds2</i>	11	13		
1 (87)	<i>D1Mit15</i>	16	8		
1 (94)	<i>Crp</i>	14	10		
1 (110)	<i>D1Mit17</i>	16	8		
1 (113)	<i>D1Mit210</i>	12	9		
2 (8)	<i>D2Mit5</i>	11	13		
2 (19)	<i>D2Mit82</i>	12	13		
2 (29)	<i>D2Mit7</i>	12	12		
2 (51)	<i>D2Mit14</i>	11	13		
2 (52)	<i>D2Mit43</i>	13	12		
2 (79)	<i>D2Mit143</i>	11	14		
2 (82)	<i>D2Mit51</i>	12	12		
2 (100)	<i>D2Mit266</i>	11	14		
3 (5)	<i>D3Mit62</i>	6	18	6.0	0.014
3 (13)	<i>D3Mit55</i>	7	18	4.8	0.028
3 (16)	<i>D3Mit21</i>	5	20	9.0	0.003
3 (17)	<i>D3Mit94</i>	6	19	6.8	0.009
3 (17)	<i>D3Mit224</i>	4	21	11.6	0.0007
3 (17)	<i>D3Mit63</i>	4	21	11.6	0.0007
3 (17)	<i>D3Mit133</i>	4	21	11.6	0.0007
3 (17)	<i>D3Mit226</i>	4	21	11.6	0.0007
3 (18)	<i>D3Mit182</i>	4	21	11.6	0.0007
3 (18)	<i>D3Mit227</i>	4	21	11.6	0.0007
3 (18)	<i>D3Mit64</i>	4	21	11.6	0.0007
3 (18)	<i>D3Mit5</i>	4	21	11.6	0.0007
3 (19)	<i>D3Mit6</i>	4	21	11.6	0.0007
3 (20)	<i>D3Mit65</i>	4	21	11.6	0.0007
3 (23)	<i>D3Mit185</i>	5	20	9.0	0.003
3 (23)	<i>D3Mit173</i>	5	19	8.2	0.004
3 (23)	<i>D3Mit7</i>	5	20	9.0	0.003
3 (23)	<i>D3Mit171</i>	5	20	9.0	0.003
3 (23)	<i>D3Mit228</i>	6	19	6.8	0.009
3 (23)	<i>D3Mit170</i>	5	20	9.0	0.003
3 (25)	<i>D3Mit154</i>	5	20	9.0	0.003
3 (27)	<i>D3Mit22</i>	6	19	6.8	0.009
3 (31)	<i>D3Mit40</i>	7	17	4.2	0.041
3 (46)	<i>D3Mit14</i>	10	15		
3 (51)	<i>D3Mit38</i>	9	13		
3 (60)	<i>D3Mit44</i>	11	12		
3 (62)	<i>D3Mit32</i>	10	12		

Continued

Table 1. Continued

Chromosome (cM) ^{2‡}	Locus	Atrophy		$\chi^2 \geq 4^{3§}$	P value
		Ho	He		
4 (9)	<i>D4Mit2</i>	13	10		
4 (34)	<i>D4Mit166</i>	14	11		
4 (34)	<i>D4Mit15</i>	14	9		
4 (51)	<i>D4Mit16</i>	14	10		
4 (68)	<i>D4Mit14</i>	12	11		
5 (16)	<i>D5Mit13</i>	14	11		
5 (18)	<i>D5Mit11</i>	12	13		
5 (27)	<i>D5Mit197</i>	13	12		
5 (46)	<i>D5Nds3</i>	12	12		
5 (47)	<i>D5Mit24</i>	11	13		
5 (53)	<i>D5Mit188</i>	10	12		
5 (64)	<i>D5Mit30</i>	14	8		
5 (76)	<i>D5Mit99</i>	13	12		
6 (21)	<i>D6Mit74</i>	14	9		
6 (13)	<i>D6Mit183</i>	14	11		
6 (26)	<i>D6Mit8</i>	13	11		
6 (40)	<i>D6Mit36</i>	12	12		
6 (54)	<i>D6Mit59</i>	14	10		
6 (64)	<i>D6Mit15</i>	13	11		
7 (9)	<i>D7Mit77</i>	12	11		
7 (19)	<i>D7Mit27</i>	12	12		
7 (30)	<i>D7Nds1</i>	13	10		
7 (55)	<i>D7Mit71</i>	15	9		
8 (13)	<i>D8Mit4</i>	13	11		
8 (36)	<i>D8Mit31</i>	11	12		
8 (55)	<i>D8Mit112</i>	15	10		
8 (69)	<i>D8Mit14</i>	11	13		
8 (74)	<i>D8Mit156</i>	11	14		
9 (14)	<i>D9Mit2</i>	14	10		
9 (35)	<i>D9Mit105</i>	13	9		
9 (41)	<i>D9Mit73</i>	15	10		
9 (44)	<i>D9Mit11</i>	16	8		
9 (52)	<i>D9Mit12</i>	13	9		
9 (57)	<i>D9Mit51</i>	14	11		
9 (67)	<i>D9Mit18</i>	14	10		
10 (3)	<i>D10Nds1</i>	11	13		
10 (10)	<i>D10Mit2</i>	14	10		
10 (13)	<i>D10Mit106</i>	14	11		
10 (41)	<i>D10Mit42</i>	14	11		
10 (50)	<i>D10Mit10</i>	14	11		
10 (67)	<i>D10Mit14</i>	14	10		

Continued

Table 1. *Continued*

Chromosome (cM) ^{2‡}	Locus	Atrophy		$\chi^2 \geq 4^{\S}$	P value
		Ho	He		
11 (5)	<i>D11Mit2</i>	12	12		
11 (26)	<i>D11Mit86</i>	2	8		
11 (37)	<i>D11Mit4</i>	12	13		
11 (49)	<i>D11Mit41</i>	10	14		
12 (4)	<i>D12Mit1</i>	13	11		
12 (7)	<i>D12Mit12</i>	12	12		
12 (34)	<i>D12Mit5</i>	11	13		
12 (60)	<i>D12Nds10</i>	10	14		
13 (9)	<i>D13Mit3</i>	14	10		
13 (28)	<i>D13Mit21</i>	9	14		
13 (46)	<i>D13Mit45</i>	9	15		
14 (11)	<i>D14Mit14</i>	10	13		
14 (31)	<i>D14Mit37</i>	13	11		
14 (49)	<i>D14Mit7</i>	13	11		
14 (67)	<i>D14Mit36</i>	14	10		
15 (6)	<i>D15Mit11</i>	14	10		
15 (8)	<i>D15Mit53</i>	10	14		
15 (18)	<i>D15Mit5</i>	8	16		
15 (34)	<i>D15Mit28</i>	12	12		
15 (61)	<i>D15Mit16</i>	14	10		
16 (0)	<i>D16Mit32</i>	7	18	4.8	0.028
16 (8)	<i>D16Mit87</i>	9	15		
16 (16)	<i>D16Mit29</i>	8	17		
16 (24)	<i>D16MIT57</i>	8	17		
16 (26)	<i>D16MIT58</i>	8	17		
16 (27)	<i>D16Mit4</i>	7	18	4.8	0.028
16 (27)	<i>D16Mit59</i>	7	18	4.8	0.028
16 (35)	<i>D16Mit5</i>	8	17		
16 (43)	<i>D16Mit19</i>	12	13		
17 (10)	<i>D17Nds3</i>	10	14		
17 (20)	<i>D17Mit10</i>	11	13		
17 (31)	<i>D17Mit20</i>	11	10		
17 (45)	<i>D17Mit2</i>	14	9		
18 (5)	<i>D18Mit20</i>	11	12		
18 (17)	<i>D18Mit24</i>	12	12		
18 (27)	<i>D18Mit9</i>	11	13		
18 (38)	<i>D18Mit4</i>	11	13		
19 (17)	<i>D19Mit16</i>	14	10		
19(28)	<i>D19Mit19</i>	16	8		
19(46)	<i>D19Mit1</i>	14	10		

Continued

Table 1. *Continued*

Chromosome (cM) ^{2‡}	Locus	Atrophy		$\chi^2 \geq 4^{\S}$	P value
		Ho	He		
X (0)	<i>DXMit55</i>	12	12		
X (27)	<i>DXMit22</i>	12	13		
X (32)	<i>DXMit25</i>	11	13		
X (32)	<i>DXMit1</i>	11	13		
X (39)	<i>DXMit16</i>	10	14		
X (42)	<i>DXNds3</i>	10	15		
X (57)	<i>DXMit36</i>	9	16		

*The atrophic phenotype was determined histologically using the 25 animals exhibiting the most severe oophoritis.

‡Markers are arranged centromeric to telomeric. Locations are as reported on the Whitehead Institute/MIT Mouse Genome Database. All are PCR-based microsatellites that distinguish C57BL/6J and A/J.

§Genotype frequency differences for atrophy were tested within the affected population by χ^2 against a predicted frequency of 1:1 for marker loci. Only $\chi^2 \geq 4$ are shown.

He, heterozygous; Ho, homozygous.

No other regions of the genome exhibited significant linkage to atrophy, suggesting that *Aod2* is the major gene controlling the development of this phenotype. This interpretation is consistent with the fact that we have covered ~94% of the total genome with an average marker locus density of 11.4 cM in our linkage analysis (Table 2). However, our results do not exclude the possible existence of one or more minor loci that we have not detected in this analysis but that might be identified using larger numbers of affected BC1 progeny and additional marker loci. In fact, the four animals exhibiting atrophy that were homozygous for all markers across the support interval are suggestive of the existence of such genes.

These mapping data place *Aod2* within a 95% confidence interval encoding two genes of particular immunologic relevance. The first is *Il2*, and the second is fibroblast growth factor basic (*Fgfb*) (15). The function of *Il2* in cell-mediated autoimmune reactions is well documented (16). However, the role of *Fgfb* in T cell-mediated inflammatory responses such as oophoritis has only recently been elaborated. Blotnick et al. (17) demonstrated that both CD4⁺ and CD8⁺ T cells synthesize and export *Fgfb*. With regard to ovarian function, *Fgfb* is mitogenic for granulosa (18) and luteal cells (19) and modulates steroidogenesis in granulosa cells (20–24), theca-interstitial cells (25), and luteal tissues (26). *Fgfb* is also present in the corpora lutea (27), luteal cells (28), and granulosa cells (29). In addition, specific high-affinity binding sites for *Fgfb* have been identified on granulosa cells (30, 31) and luteal cells (28). Such observations suggest that *Fgfb* may have an autocrine or paracrine effect on the regulation of cell growth and differentiated functions of ovarian cells (32). It is therefore not

Table 2. Percentage of Mouse Genome Covered by Exclusion Mapping*

Chromosome	Percentage of chromosome covered	Largest gap (cM)
1	92	27
2	91	27
3	100	15
4	94	25
5	100	19
6	100	14
7	93	25
8	96	23
9	99	23
10	90	28
11	77	39
12	80	27
13	97	22
14	100	20
15	89	27
16	100	15
17	100	14
18	100	12
19	100	19
X	91	27
Total	94	

*Coverage of the genome was estimated by using the position of marker loci as reported on the Whitehead Institute/MIT Mouse Genome Database and applying a value of 20 cM on each side of the marker loci.

inconceivable that *Fgfb* plays a role in the development and progression of ovarian atrophy.

Most important, however, is the co-localization of *Aod2* with *Idd3*, one of the susceptibility loci controlling autoimmune insulin-dependent type 1 diabetes mellitus (IDDM)

in the nonobese diabetic mouse (33). However, it is worth noting that the maximum support interval (from *D3Mit224*; LOD = 2.75 to *D3Mit65*; LOD = 2.75) for *Aod2* is slightly telomeric of both *Il2* and *Fgfb*. This result suggests that AOD and IDDM may share a common susceptibility gene. If, indeed, it is verified under further analysis, that *Aod2* and *Idd3* are identical, then the following conclusion is evident. Non-MHC-linked disease susceptibility genes can be divided into two distinct classes: those that play a role in multiple autoimmune diseases and those that are disease specific. MHC-linked immune response genes clearly establish a precedent for the former. Similarly, co-localization of susceptibility loci in autoimmune orchitis and IDDM has been reported (34).

The fact that ovarian atrophy is a genetically distinct component of AOD is of potential significance endocrinologically. In D3Tx mice, alterations in the plasma levels of gonadotropin hormones are observed before the development of autoimmunity (35), and similar results are seen in prenatally thymectomized nonhuman primates (36). It has been suggested that, in addition to ovarian autoimmunity, endocrinologic aberrations may also play a role in D3Tx-induced AOD. This may be through deprivation of thymic hormones and/or defective thymic-hypothalamic-gonadal regulation. It is conceivable that *Aod2* may control susceptibility to the aforementioned endocrinologic defects observed in D3Tx mice. Of particular significance with regard to potential thymus-neuroendocrine interactions, it has recently been demonstrated that a neuroendocrine signal initiated by the thymus during fetal or neonatal life is required for maturation of certain populations of T cells (37).

The identification of genes controlling AOD in mice is directly applicable to the genetic analysis of POF in humans. *Aod2* resides in the human syntenic group 4q25-q27, that is, *Il2* is at 4q26-q27 and *Fgfb* is at 4q25-q27. Similarly, the human homologue of *Aod1* resides in a syntenic group on either chromosome 3 or 22 (38). With this information, we are now in a position to ascertain whether the human homologues of these two genes play a role in the etiology of familial POF. In addition, this approach is of potential significance with regard to differential diagnosis and treatment of the disease.

We thank Julie Teuscher and William J. Griffin for their expert technical assistance.

This research was supported by National Institutes of Health grants HD21926 and HD27275 (to C. Teuscher), HD27500 (to K. S. K. Tung), and HD27506 (to S. D. Michael), National Multiple Sclerosis Society grants PP0324 and RG2659 (to C. Teuscher), and the Professional Development Fund of Brigham Young University.

Address correspondence to Dr. Cory Teuscher, Department of Microbiology, 880 WIDB, Brigham Young University, Provo, UT 84602.

Received for publication 4 May 1995 and in revised form 12 September 1995.

References

1. LaBarbera, A.R., M. Miller, C. Ober, and R.W. Rebar. 1988. Autoimmune etiology in premature ovarian failure. *Am. J. Reprod. Immunol.* 16:115–122.
2. Betterle, C., A. Rossi, S. Dalla Pria, A. Artifoni, B. Pedini, S. Gavasso, and A. Caretto. 1993. Premature ovarian failure: autoimmunity and natural history. *Clin. Endocrinol.* 39:35–43.
3. Startup, J., and V. Sele. 1973. Premature ovarian failure. *Acta Obstet. Gynecol. Scand.* 53:259–268.
4. Schwimmer, W., B. White, D. Mattison, and J.D. Schulman. 1981. Familial premature ovarian menopause: five cases in three generations. Proceedings of the 28th Annual Meeting of the Society for Gynecologic Investigation, St. Louis, MO, March 18–21.
5. Coulam, C.B., S. Stringfellow, and D. Hoefnagel. 1983. Evidence for a genetic factor in the etiology of premature ovarian failure. *Fertil. Steril.* 40:693–695.
6. Mattison, D.R., M.I. Evans, W.B. Schwimmer, B.J. White, B. Jensen, and J.D. Schulman. 1984. Familial premature ovarian failure. *Am. J. Hum. Genet.* 36:1342–1348.
7. Tung, K.S.K., S. Smith, C. Teuscher, C. Cook, and R.E. Anderson. 1987. Murine autoimmune oophoritis, epididymo-orchitis and gastritis induced by day-3 thymectomy: Immunopathology. *Am. J. Pathol.* 126:293–302.
8. Nishizuka, Y., and T. Sakakura. 1969. Thymus and reproduction: sex-linked dysgenesis of the gonad after neonatal thymectomy in mice. *Science (Wash. DC)*. 166:753–757.
9. Taguchi, O., Y. Nishizuka, T. Sakakura, and A. Kojima. 1980. Autoimmune oophoritis in mice: detection of circulating antibodies against oocytes. *Clin. Exp. Immunol.* 40:540–553.
10. Miyake, T., O. Taguchi, H. Ikeda, Y. Sato, S. Takeuchi, and Y. Nishizuka. 1988. Acute oocyte loss in experimental autoimmune oophoritis as a possible model of premature ovarian failure. *Am. J. Obstet. Gynecol.* 158:186–192.
11. Wardell, B.B., S.D. Michael, K.S.K. Tung, J.A. Todd, E.P. Blankenhorn, K. McEntee, J.D. Sudweeks, W.K. Hansen, N.D. Meeker, J.S. Griffith, et al. 1995. *Aod1*, the immunoregulatory locus controlling the abrogation of tolerance in neonatal thymectomy-induced autoimmune ovarian dysgenesis, maps to mouse chromosome 16. *Proc. Natl. Acad. Sci. USA.* 92:4758–4762.
12. Sudweeks, J.D., J.A. Todd, E.P. Blankenhorn, B.B. Wardell, S.R. Woodward, N.D. Meeker, S.S. Estes, and C. Teuscher. 1993. Locus controlling *Bordetella pertussis*-induced histamine sensitization (*Bphs*), an autoimmune disease-susceptibility gene, maps distal to T-cell receptor beta-chain gene on mouse chromosome 6. *Proc. Natl. Acad. Sci. USA.* 90:3700–3704.
13. Dietrich, W.F., J.C. Miller, R.G. Steen, M. Merchant, D. Damron, R. Nahf, A. Gross, D.C. Joyce, M. Wessel, R.D. Dredge, et al. 1994. A genetic map of the mouse with 4,006 simple sequence length polymorphisms. *Nat. Genet.* 7:220–245.
14. Lander, E.S., P. Green, J. Abrahamson, A. Barlow, M.J. Daly, S.E. Lincoln, and L. Newburg. 1987. MAPMAKER: an interactive computer package for constructing genetic linkage maps of experimental and natural populations. *Genomics.* 1:174–181.
15. Prins, J.-B., M.H. Meisler, and M.F. Seldin. 1994. Mouse chromosome 3. *Mamm. Genome.* 5:S40–S50.
16. Kroemer, G., J.L. Andreu, J. Angel, J.A. Gonzalo, J.C. Gutierrez-Ramos, and C. Martinez-A. 1991. Interleukin-2, auto-tolerance, and autoimmunity. *Adv. Immunol.* 50:147–236.
17. Blotnik, S., G.E. Peoples, M.R. Freeman, T.J. Eberlin, and M. Klagsbrun. 1994. T lymphocytes synthesize and export heparin-binding epidermal growth factor-like growth factor and basic fibroblast growth factor, mitogens for vascular cells and fibroblasts: differential production and release by CD4⁺ and CD8⁺ T cells. *Proc. Natl. Acad. Sci. USA.* 91:2890–2894.
18. Gospodarowicz, D., C.R. Ill, and C.R. Birdwell. 1977. Effect of fibroblast and epidermal growth factor on ovarian cell proliferation in vitro. I. Characterization of the response of granulosa cells to FGF and EGF. *Endocrinology.* 100:1108–1120.
19. Gospodarowicz, D., C.R. Ill, and C.R. Birdwell. 1977. Effect of fibroblast and epidermal growth factor on ovarian cell proliferation in vitro. II. Proliferative response of luteal cells to FGF but not EGF. *Endocrinology.* 100:1121–1128.
20. Mondschein, J.S., and D.W. Schomberg. 1981. Growth factors modulate gonadotropin receptor induction in granulosa cell cultures. *Science (Wash. DC)*. 211:1179–1180.
21. Baird, A., and A.J.W. Hsueh. 1986. Fibroblast growth factor as an intraovarian hormone: differential regulation of steroidogenesis by an angiogenic factor. *Regul. Pept.* 16:243–250.
22. Biswas, S.B., R.W. Hammond, and L.D. Anderson. 1988. Fibroblast growth factors from bovine pituitary and human placenta and their functions in the maturation of porcine granulosa cells in vitro. *Endocrinology.* 123:559–566.
23. Adashi, E.Y., C.E. Resnick, C.S. Croft, J.V. May, and D. Gospodarowicz. 1988. Basic fibroblast growth factor as a regulator of ovarian granulosa cell differentiation: a nonmitogenic role. *Mol. Cell. Endocrinol.* 55:7–14.
24. Oury, F., and J.M. Darbon. 1988. Fibroblast growth factor regulates the expression of luteinizing hormone receptor in cultured rat granulosa cells. *Biochem. Biophys. Res. Commun.* 156:634–643.
25. Hurwitz, A., E.R. Hernandez, C.E. Resnick, J.N. Packman, D.W. Payne, and E.Y. Adashi. 1990. Basic fibroblast growth factor inhibits gonadotropin-supported ovarian androgen biosynthesis: mechanisms(s) and site(s) of action. *Endocrinology.* 126:3089–3095.
26. Miyamoto, A., K. Okuda, F.J. Schweigert, and D. Schams. 1993. Effects of basic fibroblast growth factor, transforming growth factor- β and nerve growth factor on the secretory function of the bovine corpus luteum in vitro. *J. Endocrinol.* 135:103–114.
27. Gospodarowicz, D., J. Cheng, G.-M. Lui, A. Baird, F. Esch, and P. Bohlen. 1985. Corpus luteum angiogenic factor is related to fibroblast growth factor. *Endocrinology.* 117:2383–2391.
28. Asakai, R., K. Tamura, Y. Eishi, M. Iwamoto, Y. Kato, and R. Okamoto. 1993. Basic fibroblast growth factor (bFGF) receptors decrease with luteal age in rat ovarian luteal cells: colocalization of bFGF receptors and bFGF in luteal cells. *Endocrinology.* 133:1074–1084.
29. Neufeld, G., N. Ferrara, L. Schweigerer, R. Mitchell, and D. Gospodarowicz. 1987. Bovine granulosa cells produce basic fibroblast growth factor. *Endocrinology.* 121:597–603.
30. Baird, A., N. Emoto, A.M. Gonzalez, B. Fauser, and A.J.W. Hsueh. 1989. Fibroblast growth factors as local mediators of gonadal function. In *Growth Factors and the Ovary*. A.N. Hirshfield, editor. Plenum Press, New York. 151–160.
31. Shikone, T., M. Yamoto, and R. Nakano. 1992. Follicle-stimulating hormone induces functional receptors for basic fi-

- broblast growth factor in rat granulosa cells. *Endocrinology*. 131:1063–1068.
32. Asakai, R., S. Song, I. Nobuyuki, T. Yamakuni, K. Tamura, and R. Okamoto. 1994. Differential gene expression of fibroblast growth factor receptor isoforms in rat ovary. *Mol. Cell. Endocrinol.* 104:75–80.
 33. Wicker, L.S., J.A. Todd, and L.B. Peterson. 1995. Genetic control of autoimmune diabetes in the NOD mouse. *Annu. Rev. Immunol.* 13:179–200.
 34. Meeker, N.D., W.F. Hickey, R. Korngold, W.K. Hansen, J.D. Sudweeks, B.B. Wardell, J.S. Griffith, and C. Teuscher. 1995. Multiple loci govern the bone marrow-derived immunoregulatory mechanism controlling dominant resistance to autoimmune orchitis. *Proc. Natl. Acad. Sci. USA*. 92:5684–5688.
 35. Michael, S.D., O. Taguchi, and Y. Nishizuka. 1980. Effect of neonatal thymectomy on ovarian development and plasma LH, FSH, GH, and PRL in the mouse. *Biol. Reprod.* 22:343–350.
 36. Healy, D.L., J. Bacher, and G.D. Hodgen. 1985. Thymic regulation of primate fetal ovarian-adrenal differentiation. *Biol. Reprod.* 32:1127–1133.
 37. Wang, J., and J.R. Klein. 1994. Thymus-neuroendocrine interactions in extrathymic T cell development. *Science (Wash. DC)*. 265:1860–1862.
 38. Reeves, R.H., and M.P. Citron. 1994. Mouse chromosome 16. *Mamm. Genome*. 5:S229–S237.